Contents lists available at ScienceDirect

Physics Letters A

Spin splitter regime of a mesoscopic Rashba ring

V. Moldoveanu [a], B. Tanatar [b],*

[a] *National Institute of Materials Physics, P.O. Box MG-7, Bucharest-Magurele, Romania*
[b] *Department of Physics, Bilkent University, Bilkent, 06800 Ankara, Turkey*

ARTICLE INFO

ABSTRACT

Using the non-equilibrium Greens' function formalism we calculate the spin currents in a one-dimensional ring coupled to three leads and in the presence of perpendicular magnetic flux Φ and Rashba spin–orbit coupling. A finite bias is applied between the input lead and the other two output leads. We show that the spin–orbit coupling allows one to operate this system as a spin splitter, i.e. the output leads deliver spin-polarized currents with different orientations. We find that the spin splitter operation can be tuned at integer multiples of Φ/Φ_0. Its efficiency depends not only on the value of the Rashba coupling but also on the bias applied between the input and output leads. The selected spin orientation of the output leads can be reversed by a slight change of their contact position. We discuss as well the connection between the spin splitter operation and the spectral properties of the ring.

© 2010 Elsevier B.V. All rights reserved.

1. Introduction

Some time ago Nitta et al. [1] theoretically predicted that by varying the Rashba parameter α one could control the spin interference in a mesoscopic ring, because the spin–orbit interaction induces different Aharonov–Casher (AC) phases to different spin states. Following this idea Bergsten et al. [2] were able to measure AC oscillations in quantum ring arrays as a function of α. A lot of theoretical work has been done since, both for closed and open rings [3–7]. It was soon realized that α could be tuned such that the spin current of a given orientation is substantially suppressed while the other one is preserved. Such a device is called a spin filter [8–13]. Cohen et al. [14] calculated the conductance of molecular rings in the presence of Zeeman splitting for various contact geometries and suggested that such systems could also operate like spin filters. Most of the results on spin filters were obtained within the scattering approach to electronic transport, and therefore the relevant quantity is the spin-polarized conductance/transmittance of the ring at a *given* energy.

In a recent paper [15] we reported on the spin filter properties of a Rashba interferometer coupled to two leads and subjected to a *finite* bias. Using the non-equilibrium Greens' function formalism we calculated the spin and charge currents and discussed their Aharonov–Bohm (AB) oscillations as a function of the magnetic field and Rashba strength. The main result of that work is that the spin filter operation is effective at certain values of the magnetic field that correspond to some degeneracy points in the spectrum of the Rashba ring. Since the latter is accessible by ana-

lytical or numerical calculations, one would guess on the optimal parameters for the spin filtering.

The aim of this Letter is to complement our previous study by similar calculations of the spin-polarized currents in a three-lead Rashba ring. We focus mostly on the spin splitter properties of this system which is relatively less investigated in the literature. The idea of using the spin-dependent interference in order to operate the Rashba rings as spin splitters appeared in the work of Földi et al. [16] and states that with appropriate parameters the Rashba interference in the ring splits an unpolarized input current from lead α into spin-up and spin-down polarized components which are collected at two output leads β and γ. However their results were obtained in the absence of a magnetic field and without a finite bias between the leads. Wang et al. [17] showed through the multi-lead Landauer–Büttiker formula that the voltages on two of the leads can be tuned such that the current in the third lead is completely spin polarized. Also, Chi and Zheng [18] considered the problem of spin filtering in a three-lead ring with an embedded dot using a model Hamiltonian.

The non-equilibrium Green's function formalism allows us to analyze the splitter regime in the finite bias case. We find out that the splitter regime can be achieved even in the presence of a perpendicular magnetic field and that the selected spin orientation of the output leads can be reversed by a slight change of their contact position. As in most other approaches we do not include the effect of the electron–electron interaction which is argued to be a reasonable approximation [3].

The rest of this Letter is organized as follows. In Section 2 we briefly review the model Hamiltonian and the relevant equations, Section 3 contains the numerical results and their discussion while Section 4 is left to conclusions.

* Corresponding author.
 E-mail address: tanatar@fen.bilkent.edu.tr (B. Tanatar).

2. Model and formalism

The non-interacting electrons moving in a quasi-one-dimensional ring are described by a discretized version of the Hamiltonian proposed by Meijer et al. [19]. In the equations below, N denotes the number of sites in the ring which are indexed by an angle $\varphi_p = 2\pi p/N$, with $p = 1, \ldots, N$. In the absence of Rashba coupling the eigenfunctions of the discretized ring are easily shown to be $|\phi_l\rangle = \frac{1}{\sqrt{N}}\sum_{p=1}^{N}e^{il\varphi_p}|p\rangle$, where the orbital quantum number $l = 0, \pm 1, \ldots, \pm(N/2 - 1), N/2$ (we take N even without loss of generality). When the Rashba coupling α is included one has to introduce a local spin frame characterized by the tilt angle θ_l [3]. Let ψ_{ls} be the eigenfunctions of the Rashba Hamiltonian and $s = \pm 1$ the spin quantum number in the local spin frame. Then one can show that $|\psi_{l+}\rangle$ and $|\psi_{l-}\rangle$ are given by:

$$|\psi_{l+}\rangle = \begin{pmatrix} \cos(\frac{\theta_l}{2})|\phi_l\rangle \\ \sin(\frac{\theta_l}{2})|\phi_{l+1}\rangle \end{pmatrix}, \tag{1}$$

$$|\psi_{l-}\rangle = \begin{pmatrix} -\sin(\frac{\theta_l}{2})|\phi_l\rangle \\ \cos(\frac{\theta_l}{2})|\phi_{l+1}\rangle \end{pmatrix}, \tag{2}$$

provided that θ_l is constructed such that the off-diagonal elements of the Hamiltonian in the basis $\{\psi_{ls}\}$ vanish. Straightforward calculations lead to explicit forms for the tilt angle and for the eigenvalues E_{ls} associated to $|\psi_{ls}\rangle$. By performing the limit $N \to \infty$ we recover the expressions derived in Ref. [3]:

$$E_{l,\pm} = \hbar\omega_0\left(l - \frac{\Phi}{\Phi_0} + \frac{1}{2} \mp \frac{1}{2\cos\theta_l}\right)^2$$
$$+ \frac{\hbar\omega_0}{4}\left(1 - \frac{1}{\cos^2\theta_l}\right) \pm \frac{\hbar\omega_z}{\cos\theta_l}. \tag{3}$$

The spectral representation of the discrete rings' Hamiltonian then reads $H^R = \sum_{l,s} E_{ls}|\psi_{ls}\rangle\langle\psi_{ls}|$. Let us note that $\psi_{ls}(p\sigma) = \langle p\sigma|\psi_{ls}\rangle$ where p, p' are sites along the ring and $\sigma, \sigma' = \uparrow, \downarrow$ are spin orientations w.r.t. the z axis. In view of transport calculation one actually has to rewrite H^R in the basis $\{p, \sigma\}$, using the transformation matrix that relates the two bases (see the details in Ref. [15]):

$$H^R_{p\uparrow,p'\uparrow} = \sum_l \phi_l(p)\phi_l^*(p')\left(E_{l+}\cos^2\frac{\theta_l}{2} + E_{l-}\sin^2\frac{\theta_l}{2}\right),$$

$$H^R_{p\uparrow,p'\downarrow} = \sum_l \cos\frac{\theta_l}{2}\sin\frac{\theta_l}{2}\phi_l(p)\phi_{l+1}^*(p')(E_{l+} - E_{l-}),$$

$$H^R_{p\downarrow,p'\downarrow} = \sum_l \phi_{l+1}(p)\phi_{l+1}^*(p')\left(E_{l+}\sin^2\frac{\theta_l}{2} + E_{l-}\cos^2\frac{\theta_l}{2}\right),$$

$$H^R_{p\downarrow,p'\uparrow} = H^{R\dagger}_{p'\uparrow,p\downarrow}.$$

The spin flip processes are included in the off-diagonal parts of H^R with respect to the spin orientation: in the absence of the Rashba coupling $\theta_l = 0$ and both the Hamiltonian and Green functions become block-diagonal. The latter can be computed using the explicit form of the radial functions $|\phi_l\rangle$:

$$g^R_{p\sigma,p'\sigma'}(E) = \sum_{l,s} \frac{\psi_{ls*}(p\sigma)\psi_{ls}(p'\sigma')}{E - E_{ls} + i0}. \tag{4}$$

When the ring is coupled to one-dimensional semi-infinite leads the total Hamiltonian reads as (t_L is the hopping energy on the leads):

$$H(t) = \sum_{p,p'}\sum_{\sigma,\sigma'} H^R_{p\sigma,p'\sigma'}|p\sigma\rangle\langle p'\sigma'|$$
$$+ t_L \sum_{\nu}\sum_{n_\nu,\sigma}\left(|n_\nu\sigma\rangle\langle n_\nu + 1,\sigma| + \text{h.c.}\right)$$
$$+ \chi(t)\sum_{\nu}\sum_{\sigma}\left(V^\nu|0_\nu\sigma\rangle\langle p_\nu\sigma| + \text{h.c.}\right). \tag{5}$$

The tunneling Hamiltonian above implies a pair of sites $(0_\nu, p_\nu)$, where p_ν is the site of the ring where the lead is attached and 0_ν is the nearest site of the lead ν. We assume that the spin of the incident electron does not change at the contacts. The steady-state current entering the leads is calculated in a standard way within the non-equilibrium Green function formalism. For completeness and further discussion we give below their expressions:

$$J_\alpha = \frac{e}{h}\int_{-2t_L}^{2t_L} dE\,\text{Tr}\big\{\Gamma_\alpha G^R \Gamma_\beta G^A (f_\alpha - f_\beta)$$
$$+ \Gamma_\alpha G^R \Gamma_\gamma G^A (f_\alpha - f_\gamma)\big\}, \tag{6}$$

$$J_\beta = \frac{e}{h}\int_{-2t_L}^{2t_L} dE\,\text{Tr}\big\{\Gamma_\beta G^R \Gamma_\alpha G^A (f_\beta - f_\alpha)$$
$$+ \Gamma_\beta G^R \Gamma_\gamma G^A (f_\beta - f_\gamma)\big\}, \tag{7}$$

$$J_\gamma = \frac{e}{h}\int_{-2t_L}^{2t_L} dE\,\text{Tr}\big\{\Gamma_\gamma G^R \Gamma_\alpha G^A (f_\gamma - f_\alpha)$$
$$+ \Gamma_\gamma G^R \Gamma_\beta G^A (f_\gamma - f_\beta)\big\}. \tag{8}$$

The linewidths Γ are related to the density of states at the endpoint of the lead $\rho(E) = \sqrt{4t_L^2 - E^2}/\pi$ ($\nu = \alpha, \beta, \gamma$), i.e. $\Gamma^\nu_{p\sigma,p'\sigma'}(E) = (V^\nu)^2\delta_{pp_\nu}\delta_{p'p_\nu}\rho(E)$. In the above equations the trace means a sum over both site indices and spin indices. One then identifies the spin currents $J_{\nu,\uparrow,\downarrow}$ in each lead. Each lead is characterized by its Fermi function and the bias applied between the two leads is as usually given by the difference between their chemical potentials. Let us stress that one can choose different biases between the input and output leads. However, for simplicity we take $\mu_\beta = \mu_\gamma$ and the bias is then given by $V = \mu_\alpha - \mu_\beta = \mu_\alpha - \mu_\gamma$. We now introduce the efficiency of the spin splitter:

$$E_{\uparrow,\downarrow} = \frac{(J_{\beta,\uparrow} - J_{\beta,\downarrow})(J_{\gamma,\downarrow} - J_{\gamma,\uparrow})}{(J_{\beta,\uparrow} + J_{\beta,\downarrow})(J_{\gamma,\downarrow} + J_{\gamma,\uparrow})}. \tag{9}$$

It is clear that when $E_{\uparrow,\downarrow} = 1$ the lead β carries only spin-up current while the lead γ provides only spin-down current. The opposite situation is characterized by the efficiency $E_{\downarrow,\uparrow}$ which is defined in a similar way, by exchanging $\uparrow, \downarrow$. Let us also recall that in a two-lead geometry one has the filter efficiency defined as $F_{\uparrow,\downarrow} = J_{\uparrow,\downarrow}/(J_\uparrow + J_\downarrow)$. In the three-lead geometry one can still define $F_{\beta\uparrow}$ and $F_{\gamma\downarrow}$ in order to describe the degree of spin polarization in a given lead. We remark that a good spin filtering in one of the leads does not guarantee a good splitter efficiency.

3. Numerical results

We shall present results for a ring of radius $R = 80$ nm described by $N = 80$ sites. The hopping energy of the leads attached to the ring is $t_L = \hbar^2/2m^*a^2$, where a is the discretization constant of the ring and m^* is electron effective mass in GaAs. We take equal coupling to the leads $V^\alpha = V^\beta = V^\gamma = \tau = 0.5$.

The location of the leads is conveniently described by the angle between the three leads and the x axis as follows: for the input
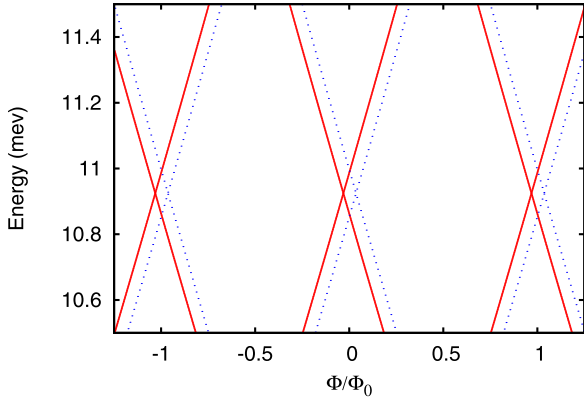
Fig. 1. (Color online.) The spectrum of a Rashba ring of radius $R = 80$ nm as a function of the magnetic flux (the Zeeman term is also included). The solid (red) lines represent the eigenvalues $E_{l,+}$ and the dotted (blue) lines are the eigenvalues $E_{l,-}$. We use $\alpha = 0.27 \times 10^{-11}$ eV m.

Fig. 2. (Color online.) (a) The splitter efficiency $E_{\uparrow,\downarrow}$ as a function of the magnetic flux (solid line) and the spin polarizations of the output leads $F_{\beta,\uparrow}$ (long-dashed line) and $F_{\gamma,\downarrow}$ (dashed line). (b) The spin currents in the output leads: solid line – $J_{\beta,\uparrow}$, long-dashed line – $J_{\beta,\downarrow}$, dashed line – $J_{\gamma,\uparrow}$, dotted line – $J_{\gamma,\downarrow}$. The angles describing the location of the output leads are $\delta = \pm 22.5°$. (c) The spin currents in the output leads for $\delta = \pm 27°$. We use the same type of lines as in (b). Other parameters: $\alpha = 0.27 \times 10^{-11}$ eV m, $\mu_\alpha = 11.5$ meV and $\mu_\beta = \mu_\gamma = 10.5$ meV, $\tau = 0.5$.

lead α which is attached to the left side of the ring the angle is fixed to π, while the output leads are located symmetrically with respect to the x axis, the corresponding angle being denoted by δ. In the numerical simulations below, $\delta > 0$ for the lead β and $\delta < 0$ for the lead γ. We also introduce the dimensionless parameter $Q_R = (\alpha/R)/\hbar\omega_0$ where $\hbar\omega_0 = \hbar^2/2m^*R^2$.

In Fig. 1 we show a part of the spectrum of the disconnected ring as a function of magnetic flux. The levels with positive (negative) slope with respect to the magnetic flux correspond to state propagating clockwise (counter clockwise) along the ring. The levels of the ring located within the bias window exhibit several crossings. A crossing between clockwise (CW) and counter clockwise (CCW) propagating states with *different* spin orientation whenever $\Phi_n = n\Phi_0/2$ (being n an integer number). The states with the *same* spin orientation in the local spin frame but propagating in opposite directions also cross at two values of the flux which are symmetrically located with respect to Φ_n. Let us mention here that the levels are computed by taking into account the Zeeman coupling.

In our previous work [15] we have shown that for a two-lead ring good filtering of up or down spin orientation can be achieved at the degeneracy points between clockwise and counter clockwise propagating states corresponding to the same spin orientation in the local spin frame of the ring. For symmetric coupling to the leads the filter efficiency is maximum around half-integer multiples of Φ/Φ_0. We argued that the spin filtering appears when the CW or CCW states interfere destructively. For asymmetric coupling we found instead that the filter operation is effective around integer multiples of Φ/Φ_0.

Let us see now what happens in the three-lead configuration. The simulations were performed for $\alpha = 0.27 \times 10^{-11}$ eV m and $\delta = \pm 22.5°$. The chemical potentials of the leads are set to $\mu_\alpha = 11.5$ meV and $\mu_\beta = \mu_\gamma = 10.5$ meV which makes the spectral region displayed in Fig. 1 the relevant one for transport. Fig. 2(a) reveals that at integer multiples of Φ/Φ_0 the splitter efficiency $E_{\uparrow,\downarrow}$ peaks up to 64% and that the spin-up/-down polarization of the lead β/γ reaches 90%. Away from these values the splitter operation is clearly ineffective as $E_{\uparrow,\downarrow}$ is very small and even vanishes at half-integer multiples of Φ/Φ_0 (the output leads actually carry unpolarized currents since $F_{\beta,\uparrow} = F_{\gamma,\downarrow} = 0.5$).

We also show in Fig. 2(b) the spin currents in the output leads over a range of one flux quanta (the currents are periodic functions of flux). This figure helps us discern the mechanism leading to the splitter regime. The maxima of the output currents are located on different sides of the degeneracy points $\Phi/\Phi_0 = 0$. At this degeneracy point $J_{\beta,\downarrow}$ and $J_{\gamma,\uparrow}$ reach their minima simulta-
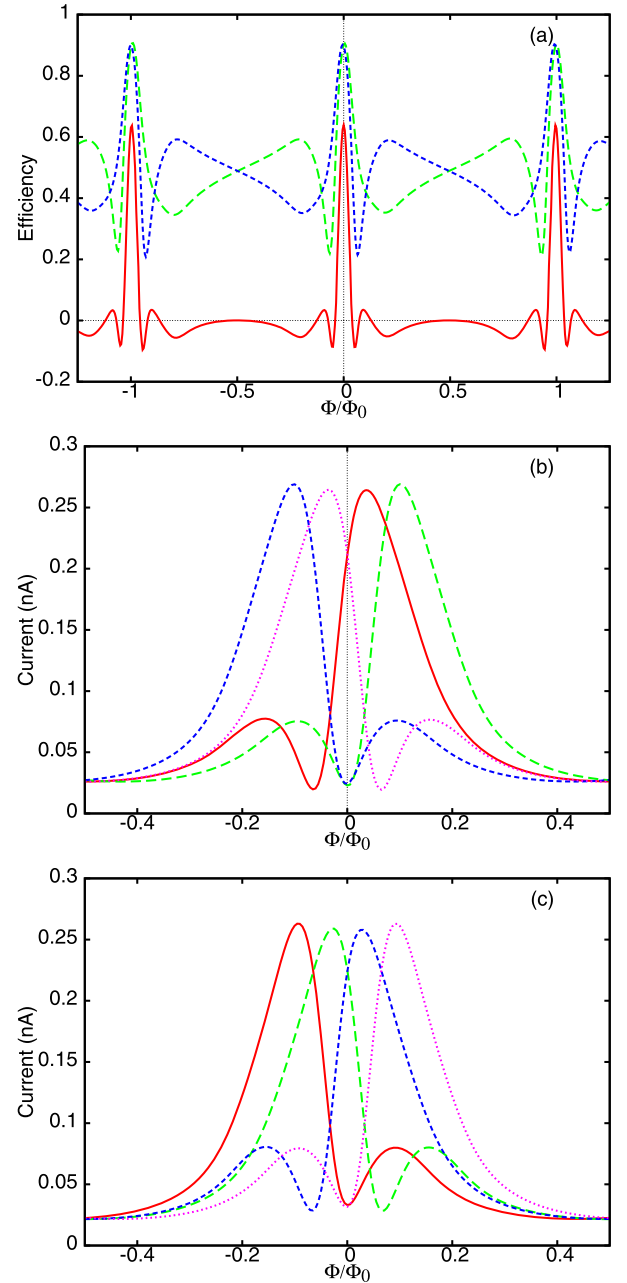
neously, while $J_{\beta,\uparrow}$ and $J_{\gamma,\downarrow}$ cross each other and have a much higher value, though not the maximum one. The splitter efficiency depends on how close is this value at the crossing point to the absolute maxima and, more importantly, on the minimum value of $J_{\beta,\downarrow}$ and $J_{\gamma,\uparrow}$ at the degeneracy point. As we shall see below, this depends on the Rashba strength and also on the bias.

The fact that the currents with different spin orientations become equal at integer multiples of Φ/Φ_0 is clearly related to the degeneracy points in the spectrum of the Rashba ring. The interference process is however far more complicated here than for the spin filter, because now the spin wavefunctions interfere at different locations (contact β and γ). For example an electron travelling

clockwise along the ring experience a first interference at the contact with the lead β and then, if it does not escape to the lead, a second interference at the contact with the lead γ is expected. The nature of this interference (mostly destructive or mostly constructive) depends essentially on the contact sites, that is, on the Aharonov–Bohm and Aharonov–Casher phases.

This sensitivity is illustrated in Fig. 2(c) showing the spin currents for the same parameters (ring radius, Rashba coupling and bias) except for the angles of the leads which are chosen $\delta = \pm 27°$. By comparing with Fig. 2(b) one notices that the spin orientations selected by the output leads are interchanged; more precisely, at $\Phi/\Phi_0 = 0$ $J_{\beta,\downarrow} = J_{\gamma,\uparrow}$ and exceed by far the other two components which drop to a minimum. In this case the relevant splitter efficiency is $E_{\downarrow,\uparrow}$. Its behavior as a function of the magnetic flux is quite similar to the one shown in Fig. 2(a), thus it is not shown.

This change in the polarization of the spin currents filtered by the output leads when the location of the latter is slightly changed confirms that the splitter regime is a consequence of quantum interference. This fact has also been reported for molecular rings by Cohen et al. [14]. It is important to point out that in that case the Zeeman coupling is more important than the Rashba coupling which is very small. For our system the situation is just the opposite: the Rashba coupling is crucial for the splitter operation.

This fact is revealed by Fig. 3(a) showing the dependence of the splitter efficiency on the parameter Q_R (which varies if the Rashba strength α varies) for different values of the bias applied between the input and the output leads. Let us discuss first the case $\mu_\alpha = 11.5$ meV and $\mu_\beta = \mu_\gamma = 10.5$ meV. The splitter efficiency corresponding to these parameters is the solid line displayed in Fig. 3(a). For small values of Q_R the output currents are not polarized and therefore the splitter efficiency is poor. As Q_R increases $E_{\uparrow,\downarrow}$ gradually improves up to 65% at a value which corresponds to $\alpha = 0.27$ and then slowly drops to zero.

In order to understand this behavior we looked at the spectrum of the ring as a function of Q_R (see Fig. 3(b)). The horizontal lines mark the chemical potentials of the leads defining the three bias windows associated to the efficiencies shown in Fig. 3(a). The spectrum corresponds to vanishing magnetic flux. At non-vanishing Q_R one notices the splitting of levels corresponding to spin-up/-down clockwise and counter-clockwise propagating states. In fact the traces in Fig. 3(b) are nothing but the 'trajectories' of the upper and lower 'corners' of the rhomboids in Fig. 1. The lifting of this degeneracy coincides with the onset of the splitter regime. Of course, there is still a degeneracy between the spin-up CW and spin-down CCW propagating states, as well as between the spin-down CW propagating and spin-up CCW states. If we select $\Phi/\Phi_0 = 1, 2 \ldots$ this degeneracy is also slightly lifted due to the Zeeman term but it does not change the behavior of the splitter efficiency.

One notices further that as Q_R increases the branches of the spectrum approach the edges of the bias window and eventually pass above and below it which implies that the total current decreases. Although it would seem that this fact is behind the drop of the splitter efficiency at larger values of α a more careful analysis shows that this is not actually the case. If the chemical potential of the input lead is increased such that the bias window covers two sets of spin states it is clear from Fig. 3(a) (see the dashed-line curve) that the splitter efficiency still drops even if there are always some levels within the bias window (i.e. the second and the third branches in Fig. 3(b)). Moreover, the maximum value of $E_{\uparrow,\downarrow}$ reduces considerably and its location does not coincide to the ones from the previous cases.

This feature is very different from the situation encountered in the spin filter case. For that system we found that the filter efficiency is quite robust with respect to the bias (see Fig. 7 from
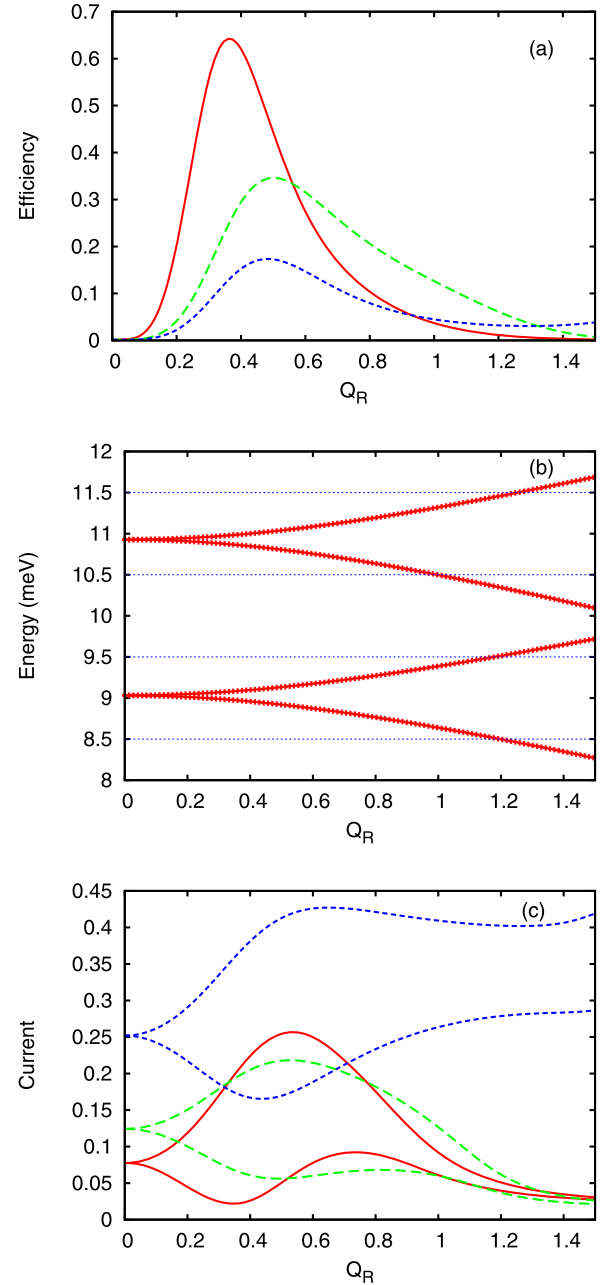

Fig. 3. (Color online.) (a) The splitter efficiency $E_{\uparrow,\downarrow}$ as a function of Q_R for different values of the bias applied on the ring. Solid line – $\mu_\alpha = 11.5$ meV and $\mu_\beta = \mu_\gamma = 10.5$ meV, long-dashed line – $\mu_\alpha = 9.5$ meV $\mu_\beta = \mu_\gamma = 8.5$ meV, dashed line – $\mu_\alpha = 11.5$ meV, $\mu_\beta = \mu_\gamma = 8.5$ meV. (b) A part of the spectrum of the ring as a function of Q_R in the absence of the magnetic flux. As Q_R (i.e. α increases) a degeneracy is lifted. As a consequence the spin currents in the output leads can be discerned. The horizontal lines mark the chemical potentials of the leads. (c) The spin currents in the output lead β at different values of the bias. The spin-up currents are always larger that the spin-down currents which also reach a minimum at a given value of Q_R. Solid line – $\mu_\alpha = 11.5$ meV and $\mu_\beta = \mu_\gamma = 10.5$, long-dashed line – $\mu_\alpha = 9.5$ meV, $\mu_\beta = \mu_\gamma = 8.5$ meV, dashed line – $\mu_\alpha = 11.5$ meV, $\mu_\beta = \mu_\gamma = 8.5$ meV.

Ref. [15]) because the destructive interference between spin-up or spin-down states always happens around half-integer multiples of Φ/Φ_0.

The main point in the spin splitter regime is a that a good efficiency $E_{\uparrow,\downarrow}$ requires small, ideally vanishing spin-down(-up) current in the lead β (γ). In Fig. 3(c) we show the currents $J_{\beta,\uparrow}$ and $J_{\beta,\downarrow}$ for the same values of the bias considered in Fig. 3(a). The solid-line curves correspond to the bias window that covers the

two levels from the top of Fig. 3(b) while the long-dashed ones are associated to a bias window covering the two lower curves in Fig. 3(b). Finally the dashed curves correspond to a larger bias that covers all the spectrum displayed in Fig. 3(a). In all cases $J_{\beta,\downarrow}$ reaches a minimum which corresponds to a maximum splitter efficiency. When the bias window covers the lowest half of the spectrum $J_{\beta,\downarrow}$ is higher than in the previous case while $J_{\beta,\uparrow}$ is smaller. Otherwise stated, the splitting between the two currents is diminished. As seen from Fig. 3(a), this implies a decrease of almost 30% in the splitter efficiency. Let us also point out that the locations of the minima of $J_{\beta,\downarrow}$ do not coincide.

Now, when the bias window is extended the currents obviously increase, because there are more levels located within it. But this also means that the minimum value that can be achieved by $J_{\downarrow,\beta}$ increases so, by its very definition, the spin splitter efficiency decreases even more. As expected, its maximum value is located in-between the maxima associated to the two cases discussed above. This does not necessarily mean that a perfect efficiency is excluded, even for a large bias. The only key to this is to find suitable parameters such that at integer multiples of Φ/Φ_0 one of the spin currents vanishes or admits very small values for consecutive pairs of levels at the *same* value of Q_R.

We find similar results for other values of the rings' radius R, although the parameters for which the splitter efficiency is maximal are also different. It is important to stress that in the present calculations the spectral properties of the ring are appropriately taken into account, in the sense that the number of sites we use to model the ring is such that the levels involved in transport (typically the lowest ones) coincide with the one of the continuous ring. We believe this to be an advantage over some simplified models which include the Rashba coupling as a phase factor in the hopping constant along the ring. Chi and Zheng [18] for example considered the problem of spin filtering in a three lead ring with an embedded dot (see also [20] for a study on rings with two quantum dots).

4. Conclusions

The spin splitter properties of a mesoscopic ring with Rashba spin–orbit coupling have been studied. The ring is coupled to one input lead and two output leads. The spin currents are calculated from the Meir–Weingreen formula and Keldysh formalism. We allow for a finite bias between the input and the output leads. We have presented numerical simulations which show that the ring can operate as a spin splitter if the perpendicular magnetic flux is an integer multiple of flux quanta. The spin polarization of the output leads can be reversed by a slight change of the location of their contacts to the ring. The dependence of the splitter efficiency on the Rashba coupling and on the applied bias is studied. When compared to the spin filter operation analyzed in our previous work [15] we find that in the splitter case the interference mechanism is more complex and therefore it is more difficult to optimize its efficiency.

Acknowledgements

References

[1] J. Nitta, F.E. Meijer, H. Takayanagi, Appl. Phys. Lett. 75 (1999) 695.
[2] T. Bergsten, T. Kobayashi, Y. Sekine, J. Nitta, Phys. Rev. Lett. 97 (2006) 196803.
[3] J. Splettstoesser, M. Governale, U. Zülicke, Phys. Rev. B 68 (2003) 165341.
[4] D. Frustaglia, K. Richter, Phys. Rev. B 69 (2004) 235310.
[5] P. Földi, O. Kálmán, M.G. Benedict, F.M. Peeters, Phys. Rev. B 73 (2006) 155325.
[6] S. Souma, B.K. Nikolić, Phys. Rev. B 70 (2004) 195346.
[7] B.K. Nikolić, L.P. Zarbo, S. Souma, arXiv:0907.4122 [cond-mat], 2009.
[8] R. Citro, F. Romeo, M. Marinaro, Phys. Rev. B 74 (2006) 115329.
[9] R. Citro, F. Romeo, Phys. Rev. B 77 (2008) 193309.
[10] P. Vasilopoulos, O. Kálmán, F.M. Peeters, M.G. Benedict, Phys. Rev. B 75 (2007) 035304.
[11] P. Lucignano, D. Giuliano, A. Tagliacozzo, Phys. Rev. B 76 (2007) 045324.
[12] Z. Zhu, Y. Wang, K. Xia, X.C. Xie, Z. Ma, Phys. Rev. B 76 (2007) 125311.
[13] S. Bellucci, P. Onorato, J. Phys. Condens. Matter 19 (2007) 395020.
[14] G. Cohen, O. Hod, E. Rabani, Phys. Rev. B 76 (2007) 235120.
[15] V. Moldoveanu, B. Tanatar, Phys. Rev. B 81 (2010) 035326.
[16] P. Földi, O. Kálmán, M.G. Benedict, F.M. Peeters, Phys. Rev. B 73 (2006) 155325.
[17] L.G. Wang, Kai Chang, K.S. Chan, J. Appl. Phys. 105 (2009) 013710.
[18] F. Chi, J. Zheng, Appl. Phys. Lett. 92 (2008) 062106.
[19] F.E. Meijer, A.F. Morpurgo, T.M. Klapwijk, Phys. Rev. B 66 (2002) 033107.
[20] F. Ming, S.-L. Liang, Chin. Phys. Lett. 25 (2008) 3389.